Online ISSN: 2981-0396 Print ISSN: 2981-0388

International Journal of Iron & Steel Society of Iran

Journal Homepage: https://journal.issiran.com/

Research Article

The Effect of the Angle of Molten Metal Exit From the Submerged Nozzle on the Flow Inside the Casting Mold

H. Safaei *[1], B. Asadi [2]

Mechanical Engineering Group, Golpayegan College of Engineering, Isfahan University of Technology, Golpayegan, Iran

ARTICLE INFO

Keywords:

Continuous casting, numerical simulation, submerged nozzle.

Article history:

Received 07 January 2025
Received in revised form 29 April 2025
Accepted 24 May 2025

ABSTRACT

Continuous casting is a vital and indispensable process in the modern steel industry, enabling efficient and large-scale production of high-quality steel. Serious challenges such as the clogging of submerged entry nozzles (SENs), however, negatively affect the process. SEN clogging, caused by the deposition of non-metallic inclusions (NMIs) or solidified steel, alters fluid flow, heat transfer mechanisms, and the overall quality of the final product. Recent advancements in computational fluid dynamics (CFD) and sophisticated experimental methods have significantly deepened our understanding on clogging dynamics. This study examines the effects of clogging-induced changes, specifically variations in jet angles, on flow patterns, vortex formation, and effective heat transfer during continuous casting. Numerical simulations based on Navier-Stokes equations and k-ε turbulence model reveal the drastic influence of jet angles on rotational flow, temperature distribution patterns, and solidification dynamics. Findings conclusively showed that a 0-degree jet angle results in stronger surface fluctuations and thicker solid shells compared to the 15-degree angle, thus improving the product quality and overall stability.

1. Introduction

Continuous casting is a critical process in the steel industry, enabling efficient production of high-quality steel products. However, issues such as the clogging of the submerged entry nozzle (SEN) challenge the process due to its significant effects on both the production efficiency and the quality of the final product.

The SEN plays an essential role in transporting molten steel from the tundish to the mold, controlling the flow path and preventing oxidation. Clogging of the SEN is primarily caused by the accumulation of solid particles, such as non-metallic inclusions (NMIs), on the inner nozzle walls [1]. This accumulation can alter the fluid flow within the mold, leading to issues such as asymmetric temperature distribution, non-uniform solidification, and reduced internal and surface quality of the final product. Different lining materials, such as mullite and spinel, exhibit various reactivity inclusions which can affect the clogging rates [2]. Clogging can also be arisen from the solidification of steel on the nozzle walls due to temperature gradients and flow conditions [1, 3].

Understanding the mechanisms underlying the

* *Corresponding Author*
Email: h.safaei@iut.ac.ir
Address: Mechanical Engineering Group, Golpayegan College of Engineering, Isfahan University of Technology, Golpayegan, Iran
1. Assistant Professor, 2. Assistant Professor

DOI: http://10.22034/IJISSI.2025.2050091.1316
Published by ISSI (Iron & Steel Society of Iran)

SEN clogging and its impact on the casting process is vital for improving both the stability and efficiency of continuous casting operations. Clogging progression can significantly alter the molten steel flow pattern, leading to surface defects or even breakouts.

Recent research has utilized computational fluid dynamics (CFD) models and experimental methods to enhance the understanding of SEN clogging, detection techniques, potential prevention strategies, and the impact of clogging on flow patterns and heat transfer in the mold.

Based on Rackers and Thomas [4] and Bai and Thomas [5], nozzle clogging can reduce the melt flow rate, leading to a decreased heat transfer rate within the mold. This can result in non-uniform solidification shell formation, raising the risk of surface breakouts in the final product. Conversely, abrupt changes in flow patterns due to the fracture and detachment of deposits from the nozzle surface can result in significant fluctuations in heat transfer and create surface defects in the product. Barati et al. [6] proposed a transient numerical model for effective simulation of the clogging process in submerged entry nozzles (SEN) during steel continuous casting, capturing both the early and late stages of clogging. This study underscores the influence of non-metallic inclusions (NMIs) in the clogging process, emphasizing their role in the formation and growth of clogs due to turbulent melt flow. The findings reveal that clogging initiates at the bottom and ports of the SEN, with fragmentation primarily occurring in the port area, which is critical in understanding the flow dynamics and clog management. The evolution of clogging leads to significant changes in flow patterns within the SEN, including the formation of vortices that affect the clogging process and the overall melt flow behavior. Li et al. [7] characterized the clogging process in submerged entry nozzles (SEN) as a dynamic phenomenon rather than a static one, wherein fragments of the obstruction can detach and be carried away by the steel flow. These dislodged particles may either become entrapped within the solidifying steel, resulting in inclusions which degrade the quality of the final product, or ascend to the top, altering the composition of the mold flux. Both scenarios pose significant challenges in retaining the product integrity. Moreover, as clogging intensifies, the restricted flow space within the SEN leads to an increase in flow velocities at its outlet, further complicating the casting process.

Concerning the heat transfer, nozzle clogging can significantly change the temperature distribution and heat flux in the mold. This, in turn, can affect the solidification process and consequently, the microstructure and mechanical properties of the final product. Numerical simulations by Pfeiler et al. [8] demonstrated that changes in the internal geometry of the nozzle due to clogging can alter the rotational and turbulent flow patterns in the mold, which can influence heat and mass transfer in the casting process.

One notable aspect of clogging is its effect on the angle of the molten jet exiting the nozzle. The changes in jet angle can significantly influence the flow and heat transfer within the mold. The present study aims to examine the effect of these jet angle on the flow dynamics and heat transfer of the molten material, offering new insights into how clogging-induced changes can be mitigated to improve casting quality.

2. Mathematical Model

Numerical simulation of the casting process is a challenging problem in computational fluid dynamics. The fluid flow, liquid-solid phase change, and other factors further add to computational complexities. Computational models must be able to accurately simulate fluid flow, temperature, and the thickness increase of the solidifying steel shell. The transient energy equation must be solved to obtain the slab temperature. Therefore, it is necessary to solve the full Navier-Stokes equations in the turbulent flow regime with proper source term to include phase changes.

2.1. Governing Equations

The equations employed in this section were previously validated and utilized by the authors [9].

The continuity equation for any incompressible fluid flow is given by:

$$\vec{\nabla}.\vec{V} = 0 \qquad \text{Eq.(1)}$$

Where $\vec{V}$ is the velocity vector of the fluid flow. The momentum equation in its general form can be derived by:

$$\frac{\partial(\rho\vec{V})}{\partial t} + \vec{\nabla}.(\rho\vec{V}\vec{V}) = -\vec{\nabla}p \qquad \text{Eq.(2)}$$

$$+\vec{\nabla}.\left(\mu\vec{\nabla}\vec{V}\right) - \vec{g}\cdot\vec{x}\nabla\rho + \vec{S}_v$$

Here, $\vec{S}_v$ denotes the source term for solidification. This term must ensure that as the steel solidifies, its velocity reduces to 0. The source term was defined by Voller [10] as:

$$\vec{S}_v = -A\vec{V} \quad where \quad A = \frac{-C(1-\theta)^2}{(\theta^3+\varepsilon)} \qquad \text{Eq.(3)}$$

Where θ is the liquid fraction of the computational cell whose determination method is further explained in the energy equation. The parameter C depends on the

morphology of the porous medium, while ε is a small value added to the denominator to prevent numerical instability.

The k-ε turbulence model is employed to simulate turbulent flow while the energy equation must be utilized for modeling heat transfer effects and tracking the phase change boundary:

$$\frac{\partial(\rho C_p T)}{\partial t} + \vec{\nabla}\cdot(\rho C_p \vec{V} T) \quad \text{Eq.(4)}$$

$$+\left(\frac{\partial \rho K_E}{\partial t} + \vec{\nabla}\cdot(\rho \vec{V} K_E)\right)$$

$$= -\frac{\partial P}{\partial t} + \vec{\nabla}\cdot(k\vec{\nabla}T)$$

$$+\vec{\nabla}\cdot\left(\underset{\sim}{\tau}\cdot\vec{V}\right) + \rho\vec{g}\cdot\vec{V} + S_h,$$

$$S_h = \frac{\partial \rho \Delta H}{\partial t} + \vec{\nabla}\cdot(\rho\vec{V}\Delta H)$$

$$\underset{\sim}{\tau} = \mu\left[\vec{\nabla}\vec{V} + \vec{\nabla}\vec{V}^T\right] - \frac{2}{3}\mu I\vec{\nabla}\cdot\vec{V}$$

Where K_E is kinetic energy of the fluid, $\underset{\sim}{\tau}$ represents the stress tensor, k is the thermal conductivity, S_h is the solidification source term and ΔH is the latent heat of fusion.

Voller [10] assumed that in the mushy zone, the latent heat of fusion ΔH is a fraction of the total latent heat of solidification L, expressed as ΔH = θL. Rösler [11] proposed the following function for θ:

$$\theta = 0.5 erf\left(\frac{4(T - T_m)}{(T_l - T_s)}\right) + 0.5 \quad \text{Eq.(5)}$$

In which, T_l represents the liquidus temperature, T_s denotes the solidus temperature, and T_m shows the average of T_l and T_s. Consequently, the energy equation transforms into the form expressed in Equation (6):

Eq.(6)

$$\frac{\partial(\rho C_p T)}{\partial t} + \vec{\nabla}\cdot(\rho C_p \vec{V} T)$$
$$+\left(\frac{\partial \rho K_E}{\partial t} + \vec{\nabla}\cdot(\rho \vec{V} K_E)\right)$$
$$= -\frac{\partial P}{\partial t} + \vec{\nabla}\cdot(k_{eff}\vec{\nabla}T)$$
$$+\vec{\nabla}\cdot\left(\underset{\sim}{\tau}\cdot\vec{V}\right) + \rho\vec{g}\cdot\vec{V} + S_h where$$

$$S_h = -\rho L \frac{4\cdot\left(\left(\frac{4(T - T_m)}{(T_l - T_s)}\right)^2\right)}{(T_l - T_s)\sqrt{\pi}}\cdot\left(\frac{\partial T}{\partial t} + \vec{V}\cdot\vec{\nabla}T\right)$$

2.2. Boundary conditions

Molten steel flows into the mold through a submerged entry nozzle (SEN). As an inlet boundary condition for this region, the mass flow rate is specified. The inlet mass flow rate can be determined based on the casting speed, the cross-sectional area of the steel strand, and the outlet cross-sectional area of the nozzle. The casting speed in the present study is 1 m/min. No-slip condition was applied to the solid walls of the mold. If a solidified shell forms on the mold wall, it is assumed to move downwards at the casting speed. The primary cooling of the steel strand takes place within the mold by circulating water through four faces/panels. Based on the flow rate and temperature change of the cooling water, the average cooling rate in this region can be estimated as follows:

$$\overline{q} = \frac{C_{pw} Q_m \mathrm{D}T}{S_{eff}} \quad \text{Eq.(7)}$$

Where C_{pw} is the specific heat capacity of water, Q_m denotes the water flow rate, ΔT represents the difference in the inlet and outlet water temperatures, and S_{eff} [5] stands for the effective contact area between the mold and the steel. The heat flux distribution along the mold is such that, as the casting progresses, the heat flux decreases, with the maximum heat flux observed at the beginning of the mold. The heat flux distribution can be described by:

$$q = 2680000 - \beta\sqrt{\frac{L}{u_{cast}}} \quad J/m^2 s \quad \text{Eq.(8)}$$

Where:

$$\beta = \frac{1.5\left(2680000 - \overline{q}\right)}{\sqrt{\frac{L}{u_{cast}}}} \quad \text{Eq.(9)}$$

L represents the distance from the free surface of the melt within the mold, while L_m denotes the mold length. For free surfaces, the zero-shear stress condition is imposed. Radiation from these surfaces occurs with an emissivity of 0.8. A zero-shear stress boundary condition was applied at the top surface of the mold; i.e. the molten metal-air interface.

3. Results and Discussion

This section addressed the simulation of the fluid flow and heat transfer rate. To verify the accuracy and reliability of the numerical solution, the simulation results were compared and validated with the numerical findings of Shamsi and Ajmani [12].

The solidification length can be considered the most important parameter for comparing the results of the aforementioned study with the present research. The

solidification length of Shamsi [12] and the present research were found to be 19.3 and 19.6 m, respectively, with only a 0.3-meter difference. Fig. 1. compares the temperature variations at the center of the slab. The results from both studies exhibit minor discrepancies, thereby validating the accuracy of the current simulation.

Fig. 2. shows a schematic of the computational domain.

The slab thickness is 200 mm. Due to the symmetry of the problem, only half of the solution domain was modeled. The properties of steel and the values used in the numerical simulation are presented in Table 1.

Fig. 3. illustrates the velocity variations in the mold region at exit angles of 0 and 15°.

After exiting the nozzle, the liquid metal jet is directed towards the narrow part of the mold. As a consequence of jet expansion, the velocity experiences a reduction in the forward direction. On the other hand, the impact of the jet on the wall increases the velocity of the melt near the wall.

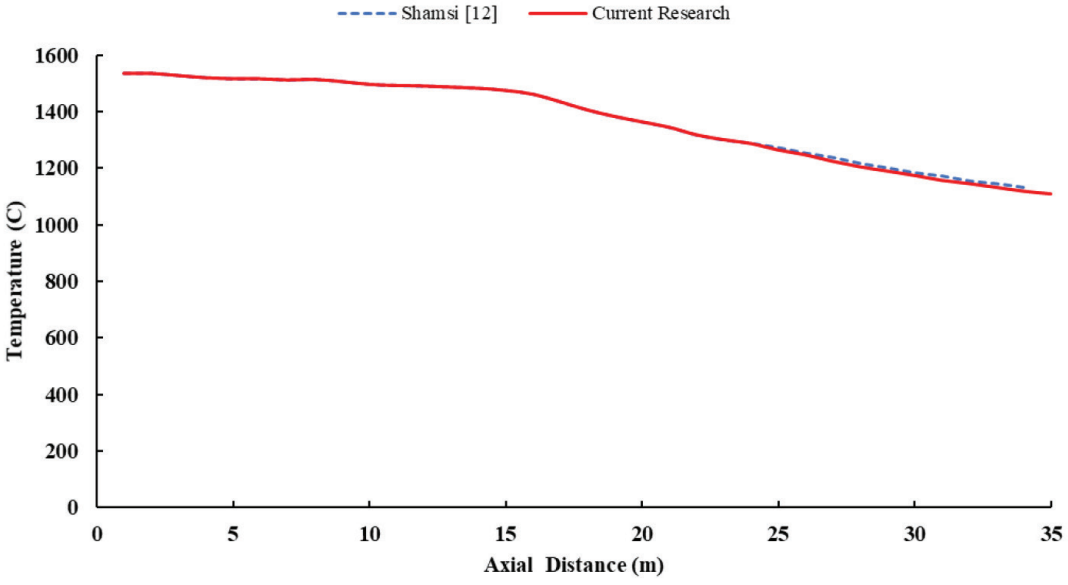

Fig. 1. Comparison of temperature variations along the line passing through the surface center of the slab in the present study and Shamsi's research [12].

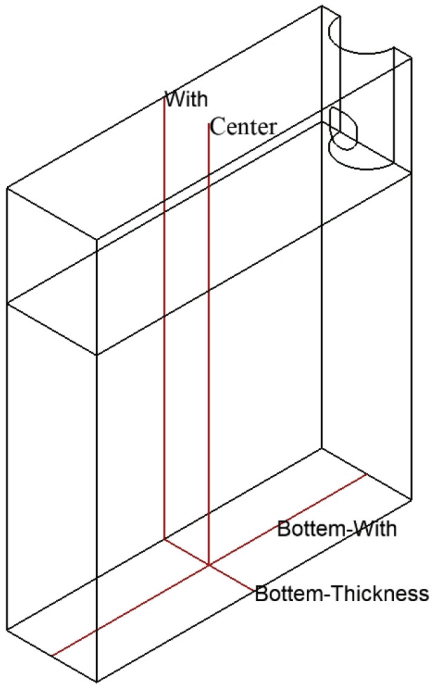

Fig. 2. Schematic of the computational domain.

Table 1. Properties of steel and values used in the numerical simulation.

Thermal conductivity of steel (W/m.K)	34.6
Viscosity of steel (kg/m.s)	0.0062
Latent heat of solidification (J/kg)	271954
Solidus temperature ($^{\circ}C$)	1496
Liquidus temperature ($^{\circ}C$)	1529
Melt superheat ($^{\circ}C$)	24
Specific heat of steel ($J/kg.^{\circ}C$)	682
Length of the casting mold (m)	0.85
Strand cross-sectional area ($\mathrm{m}\times\mathrm{m}$)	1.4×0.2
SEN diameter (m)	0.12

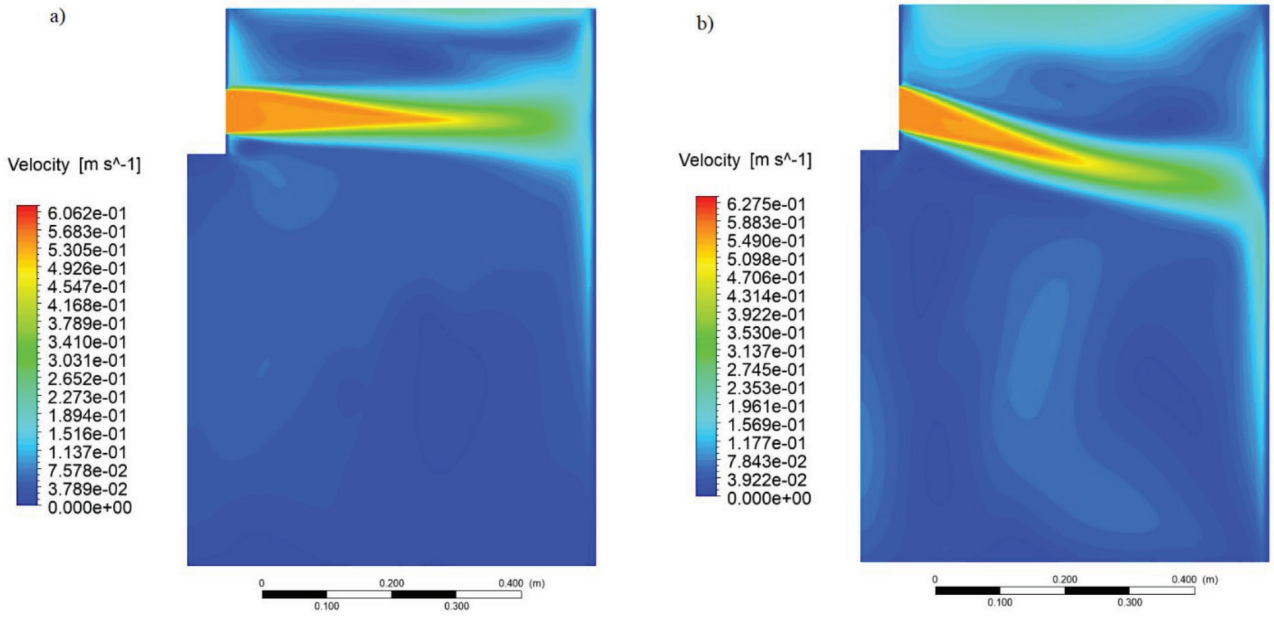

Fig. 3. Velocity variation contours in the mold: (a) 0-degree angle, (b) 15-degree angle.

The interaction of the jet with the wall, in conjunction with the movement of the fluid, gives rise to the formation of rotational regions both above and below the jet (Fig. 4).

The upper rotation is stronger due to its proximity to the free surface. The velocity and rotational flow in the lower part of the mold are also significant, even at a distance of 0.5 m below the mold. The flow becomes almost uniform after this region.

As seen in Fig. 5. the flow pattern is quite different for the two impact angles. At a 0-degree angle, a strong rotational region is formed above the jet and a weak rotational region below it. However, at a 15-degree impact angle, one vortex is formed above the jet while two vortices are located below the jet. The maximum velocity at the upper surface is 0.45 and 0.3 m/s at the 0-degree and 15-degree angle cases, respectively. This implies higher strength of the upper vortex at the 0-degree angle than at the 15-degree angle, leading to more surface fluctuations at the 0-degree angle. More fluctuations at the interface can trap argon gas bubbles in the upper slag layer.

Fig. 5. shows the pressure variations at two impact angles.

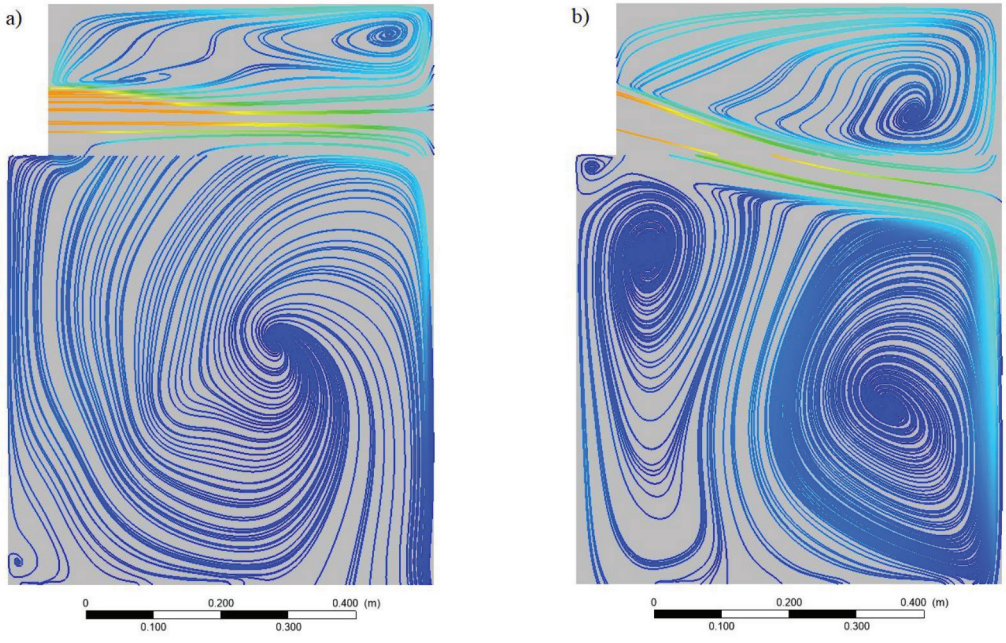

Fig. 4. Streamlines and vortex formation in the mold: (a) 0-degree angle, (b) 15-degree angle.

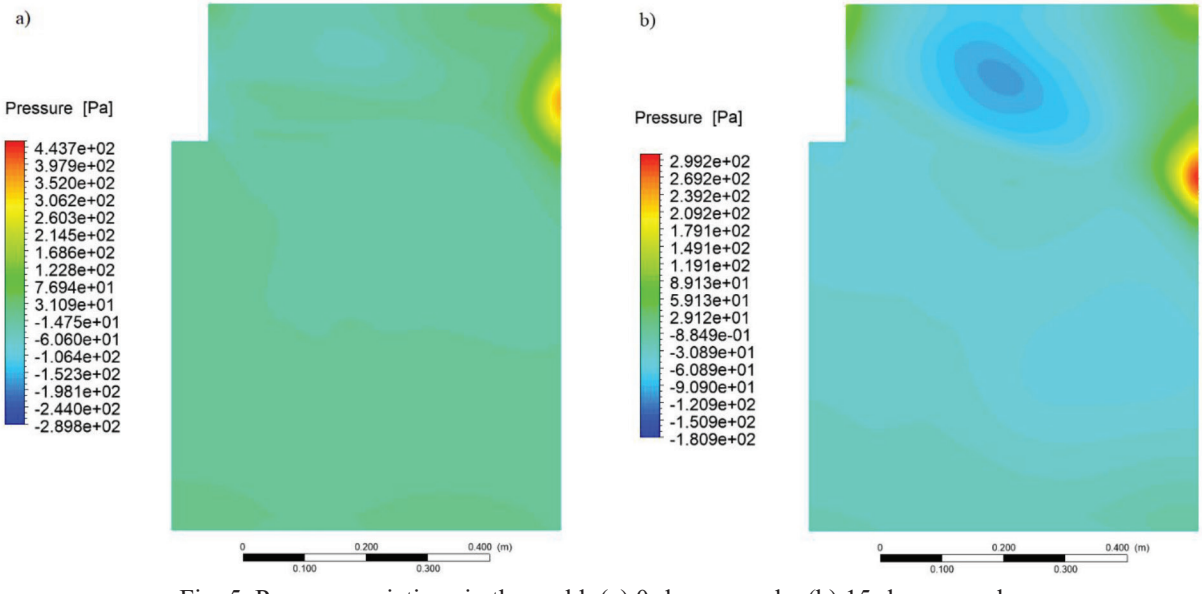

Fig. 5. Pressure variations in the mold: (a) 0-degree angle, (b) 15-degree angle.

As can be seen, the pressure at the stagnation point is 437 and 299 Pa at the 0-degree and 15-degree angle cases, respectively. Such a pressure can cause the slag layer to rupture at the vertical wall of the mold. If the slag layer is lost, the molten steel adheres to the mold wall, increasing the probability of the breakout phenomenon.

Fig. 6. shows the temperature variations at the mold exit and in the direction of the longer side of the mold.

Accordingly, the temperature drop is very high near the shorter side of the mold due to the presence of water circuits in the mold and initial cooling. This temperature drop is such high that a solid shell is formed near the mold wall. Fig. 7. illustrates the variations in the liquid fraction along the line Bottom-With shown in Fig. 2.

According to Fig. 7. the thickness of solid shell is about 20 and 5 mm for the 0-degree and 15-degree angle cases, respectively. At the 0-degree angle case, the lower vortex is weaker that the 15-degree angle, and the melt can exchange heat with the wall better. The presence of this solid shell is necessary as it holds the superheated liquid in its center. If, for any reason, this shell does not reach the appropriate thickness and the breakout occurs [2], it will cause significant damage to the casting machine.

4. Conclusions

This study highlights the dynamic nature of SEN clogging and its implications for continuous casting. Numerical simulations demonstrated that clogging-induced changes in jet angles critically affect the flow behavior, temperature distribution, and solidification patterns. Stronger near-surface vortices and thicker solidified shells were observed in the case of the 0-degree jet angle, which mitigate breakout risks but increase surface fluctuations. Conversely, a 15-degree angle exhibited reduced surface disturbances but thinner shells, heightening breakout risks. These findings underscore the need for optimized flow control strategies to balance solidification stability and surface quality.

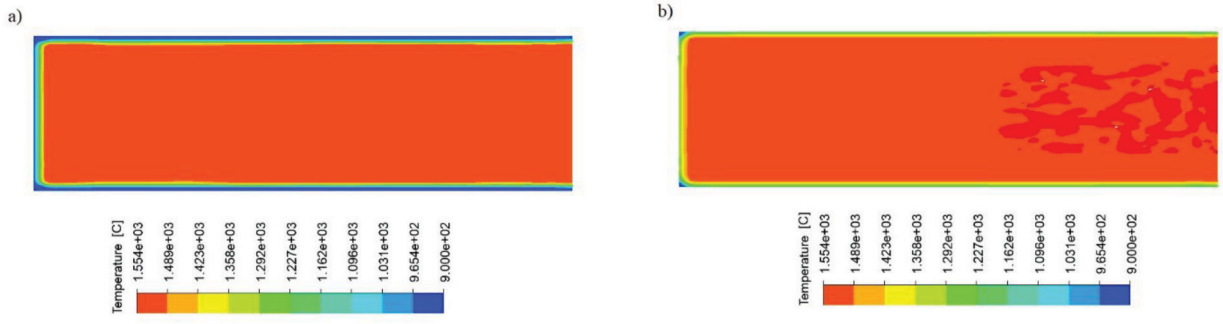

Fig. 6. Temperature variations at the mold outlet: (a) zero-degree angle, (b) 15-degree angle.

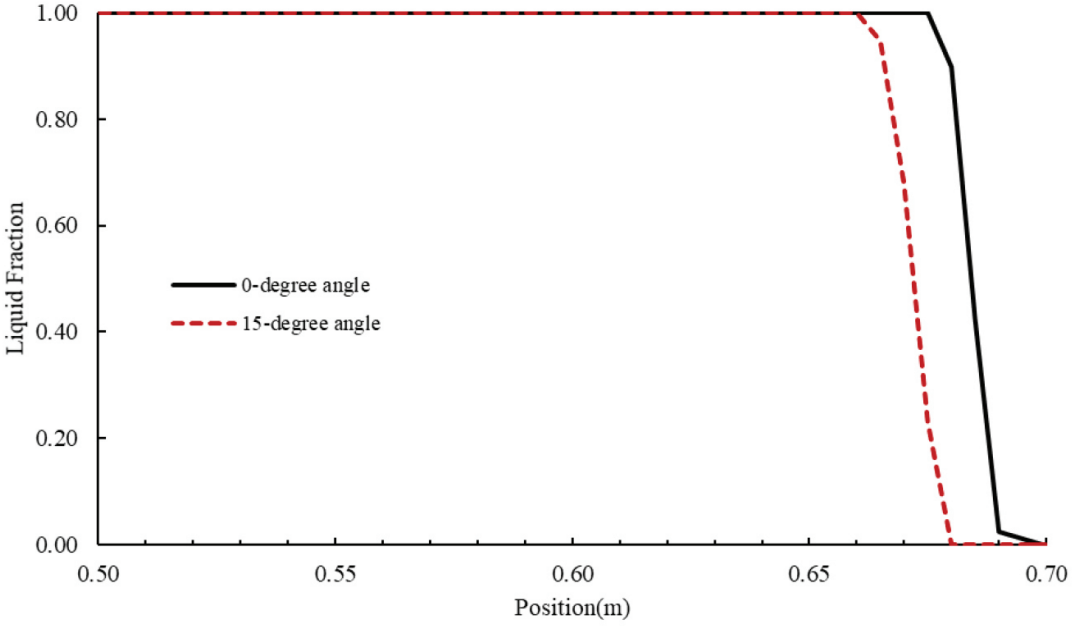

Fig. 7. Liquid fraction variations at the mold outlet: (a) 0-degree angle, (b) 15-degree angle.

Future research are recommended to address the modification of the CFD models to include real-time clogging dynamics and experimental validation to improve industrial casting processes.

References

[1] Barati H, Wu M, Kharicha A, Ludwig A, Role of solidification in submerged entry nozzle clogging during continuous casting of steel, Steel Res Int. 2020; 91(12): 2000230.

[2] Ma F.X, Zhang Y, Liu S, Wang J, Chen Z, et al. A systematic study of carbon-free oxide-based lining for preventing submerged entry nozzle clogging in continuous casting of rare earth steel, J Iron Steel Res Int. 2024; 1–12.

[3] Vakhrushev A, Sorokin A, Eremin A, Kirsanov V, Lvov I, et al. On modelling parasitic solidification due to heat loss at submerged entry nozzle region of continuous casting mold, Metals. 2021; 11(9): 1375.

[4] Rackers K, Thomas B, Clogging in continuous casting nozzles. In: Steelmaking conference proceedings, Warrendale (PA): Iron and Steel Society of AIME. 1995.

[5] Bai H, Thomas B.G, Turbulent flow of liquid steel and argon bubbles in slide-gate tundish nozzles: Part I, model development and validation, Metall Mater Trans B. 2001; 32: 253–67.

[6] Barati H, Wu M, Kharicha A, Ludwig A, Transient simulation of melt flow, clogging, and clog fragmentation inside SEN during steel continuous casting. In: IOP Conf Ser Mater Sci Eng. 2023. Bristol (UK): IOP Publishing.

[7] Li Y, Zhang J, Wang X, Liu Y, Yang Q, et al. Mathematical modeling of transient submerged entry nozzle clogging and its effect on flow field, bubble distribution and interface fluctuation in slab continuous casting mold, Metals. 2024; 14(7): 742.

[8] Pfeiler C, Wu M, Ludwig A, Influence of argon gas bubbles and non-metallic inclusions on the flow behavior in steel conti=nuous casting, Mater Sci Eng A. 2005; 413: 115–20.

[9] Safaei H, Emami M.D, Jazi H.S, Mostaghimi J, Application of compressible volume of fluid model in simulating the impact and solidification of hollow spherical ZrO_2 droplet on a surface, J Therm Spray Technol. 2017; 26: 1959–81.

[10] Voller V.R, Prakash C, A fixed grid numerical modelling methodology for convection-diffusion mushy region phase-change problems, Int J Heat Mass Transf. 1987; 30(8): 1709–19.

[11] Rösler F, Brüggemann D, Shell-and-tube type latent heat thermal energy storage: numerical analysis and comparison with experiments, Heat Mass Transf. 2011; 47(8): 1027–33.

[12] MRRI S, Three dimensional turbulent fluid flow and heat transfer mathematical model for the analysis of a continuous slab caster, ISIJ Int. 2007; 47(3): 433–42.